Parametric Study of a Ball-Screw Energy Harvester Shock Absorber

Hajar Djellal [1*], *Biagio* Morrone[1], *Luigi* Costanzo[1], *Massimo* Vitelli[1] and *Aouatif* Saad[2]

[1]Department of Engineering, Università della Campania "L. Vanvitelli", Aversa 81031 -ITALY
[2]Advanced Systems Engineering Laboratory (ASELab), National School of Applied Sciences, Ibn Tofail University, Kenitra 14000 - MOROCCO

Abstract. This paper investigates a ball-screw energy harvester shock absorber (BS-EHSA) equipped with a DC motor/generator and driven by an external sinusoidal force. A comprehensive parametric study examines the effect on the power delivered to the load of varying the sprung mass, external electrical resistance, and spring constant. A simulation study is also performed to demonstrate how the resonance frequency of the system impacts energy recovery. Numerical simulations are carried out in the MATLAB environment, providing insights into optimizing system parameters for maximum power efficiency.

1 Introduction

Amidst diminishing natural resources, our dependence on renewable energy and energy-efficient technologies is increasing. With the substantial increase in energy consumption, there is a significant move from conventional internal combustion engine cars to electric vehicles [1]. Nevertheless, electric vehicles face challenges such as limited range and need for numerous batteries, increasing both cost and weight, which raise both expenses and burden. One possible approach involves harnessing energy from the suspension system by converting vibration energy into electrical energy. Previously wasted as heat from shock absorbers, this energy can now be efficiently harvested [2].

Many Energy Harvester Shock Absorber (EHSA) designs, such as rotating and linear electromagnetic harvesters, have been developed and tested [3]. Whereas in a rotary-based electromagnetic harvester the vertical vibrations are translated into rotational motions of the generator, producing electrical energy, in a linear electromagnetic harvester, the kinetic energy of the vertical oscillations is directly converted into electrical energy through electromagnetic induction without the need for transmission mechanisms.

Zhou et al. [4] proposed magnetic energy harvesting and studied the influencing factors on the energy harvesting characteristics under various excitations to validate the use of the harvested energy in self-powered sensing. In order to increase the efficiency of electric buses and to capture energy from uneven road profiles, an energy regenerative shock absorber (ERSA) was developed by Abdelrahman et al. [5] based on a slotted link conversion mechanism to transform linear vibrations into unidirectional rotations of the generator shaft for energy harvesting. A high efficiency regenerative shock absorber was proposed by Zhang et al. [6] made of paired ball screw with gears assembly and dual overrunning clutches to transform bidirectional movement into unidirectional one. Besides recovering the energy from the generator and storing it in capacitors, the regenerative shock absorber can minimize the vibration induced by uneven roads and enhance driving comfort.

Zhang et al. [7] proposed a novel energy harvester suspension based on hydraulic transmission comprising a hydraulic system connected with a hydraulic motor generator. Energy conversion efficiency can reach 40.4% under the external resistance of 5 Ohm.

The current paper presents a basic EHSA system that includes a ball screw mechanism linked with a DC motor/generator connected to a pure resistive load. This study aims to explore and analyze the energy recovery potential of the proposed EHSA, focusing on how the adjustment of system parameters such as load resistance, spring constant and sprung mass influence its performance. In addition, it seeks to examine the effects of resonance frequency in the suspension system and its implications for power output.

2 System Description and Modeling

Numerous models rooted in Newtonian physics and conservation principles have been utilized in the literature to study the dynamics, behavior, and the performance of car suspensions. In this context, one common and basic approach is to represent the suspension system as a 1-DOF (Degree of Freedom) using a quarter-car model, like the one shown in Fig.1

* Corresponding author: hajar.djellal@unicampania.it

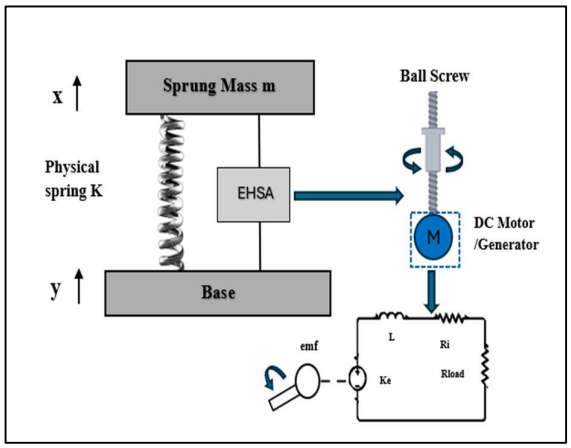

Fig. 1. Quarter-car Model: 1-DOF model and the basic electric circuit.

The regenerative suspension system consists of three main parts: a ball screw mechanism, a planetary gearbox, and a DC permanent magnet rotary machine. Given that the generator's (motor's) inductance is very small in relation to resistance, the impact of the generator's internal inductance can be disregarded. The performance of each of these parts can be explained from two perspectives: energy recovery and damping. From an energy regeneration perspective, the ball screw mechanism converts translational motion due to road roughness into a rotary motion. Then the planetary gearbox increases the rotary motion amplitude, resulting in a higher voltage at the output of the generator.

According to [8-9], the equations of the dynamics of the system below are used to develop the equivalent mechanical model.

The motor output torque, τ_i, is expressed as a function of the current flowing through the load resistor R_{load}, I, as:

$$\tau_i = k_t I = \frac{k_t V_{emf}}{R_{\text{int}} + R_{load}} \tag{1}$$

where R_{int} is the internal resistance and V_{emf} is the back EMF voltage generated by motor rotation and is defined as follows:

$$V_{emf} = k_e k_g \eta_g \dot{\theta} \tag{2}$$

with k_t, k_e and k_g being the torque constant, the back EMF coefficient of DC motor and the gear ratio of the gearhead respectively, being η_g the efficiency of the gearbox mechanism and $\dot{\theta}$ the angular velocity of the generator.

The equation of the rotor dynamics is given by:

$$\tau_b = \frac{k_e k_t k_g^2 \eta_g^2}{R_{\text{int}} + R_{load}} \dot{\theta} + (J_m k_g^2 \eta_g^2 + J_g + J_b)\ddot{\theta} \tag{3}$$

Where J_m, J_g and J_b are respectively the inertias of motor, gearbox and ball screw.

Based on the characteristics of the ball screw mechanism, the relationship between the output torque and force, as well as between angular motion and linear stroke, is given by:

$$\tau_b = d\eta_b F_b \quad , \quad \theta = \frac{z}{d\eta_b} \tag{4}$$

where d is the coefficient of transformation of the ball screw, η_b is the efficiency of ball screw, F_b is the output force of the ball screw and z is the stroke displacement of the shock absorber.

When the ball screw's non-linearities are ignored [8], the equivalent output force of the damper is given by:

$$F_b = \frac{k_e k_t k_g^2 \eta_g^2}{(R_{\text{int}} + R_{load}) d^2 \eta_b^2} \dot{z} + \frac{(J_m k_g^2 \eta_g^2 + J_g + J_b)}{d^2 \eta_b^2} \ddot{z} \tag{5}$$

The suspension system's dynamic equation can be stated as:

$$m_{eq}\ddot{z} + c_{eq}\dot{z} + kz = m\omega^2 A \sin(\omega t) \tag{6}$$

where:

$$m_{eq} = m + \frac{J_m k_g^2 \eta_g^2 + J_g + J_b}{d^2 \eta_b^2} \tag{7}$$

Considering that friction and backlash are comparatively small compared to other transmission systems

$$c_{eq} = \frac{k_e k_t k_g^2 \eta_g^2}{(R_{\text{int}+} R_{load}) d^2 \eta_b^2} \tag{8}$$

Based on Equation (6), the parameters that intervene in the system dynamic equation are reported in Table 1.

Table 1. Ball-screw EHSA parameters and values [8].

Parameters	Value
Total spring constant soft (k_{soft})	10795 N/m
Total spring constant hard (k_{hard})	73320 N/m
Rotor inertia of the DC motor (J_m)	120 g cm^2
Torque constant of the DC motor (k_t)	170 mN m/A
Back EMF coefficient of the DC motor(k_e)	170 mV/rad/s
Internal resistance of the DC motor (R_{int})	10.2 Ω
Rotor inertia of the gearhead (J_g)	17.6 g cm^2
Gear ratio of the gearhead (k_g)	12:1
Efficiency of the gearhead (η_g)	83%
Rotor inertia of the ball screw (J_b)	1248 g cm^2
Lead ratio of the ball screw (l)	60 mm/r
Efficiency of the ball screw(η_b)	95%

In the context of an energy harvesting system, the performance of an EHSA has a considerable influence on driving comfort and regenerated power. According to ISO 2631-1, vibrations in the frequency range from 0.5 Hz to 80 Hz can affect driving comfort [10]. Thus, the resonant frequency is crucial in this context.

The harnessed power is divided into three primary parts: mechanical dissipation, electrical loss, and power provided to the electrical load. Maximizing the power delivered to the electrical load is crucial for capturing useful power effectively. The average power delivered to the load is calculated as:

$$P_{avg} = I^2 R_{load} = \frac{k_e^2 k_g^2 R_{load}}{(R_{\text{int}} + R_{load})^2 d^2 \eta_b^2} \dot{z}^2 \quad (9)$$

A parametric study on the energy regenerated from BS-EHSA is carried out. The simulation forced the system to vibrate by producing the resonant frequency response for different values of sprung masses, in the range 16 kg – 600 kg, over a large range of frequencies with base excitation amplitude of 10 mm. Two types of spring were simulated: one with a soft value of the spring constant, k_{soft} = 10795 N/m, and the other with a hard value, k_{hard} = 73320 N/m, in addition to variable resistive loads ranging from 10 Ω to 490 Ω, representing the external load of the electrical generator.

3 Results and Discussions

According to equation (8), the equivalent damping coefficient c_{eq} is significantly influenced by the external electrical load R_{load}. By varying the external resistance from 10 Ω to 490 Ω, the damping coefficient ranged from 1724.55 N s/m to 69.64 N s/m. Fig.2 shows the impact of external resistance variation on the equivalent damping coefficient.

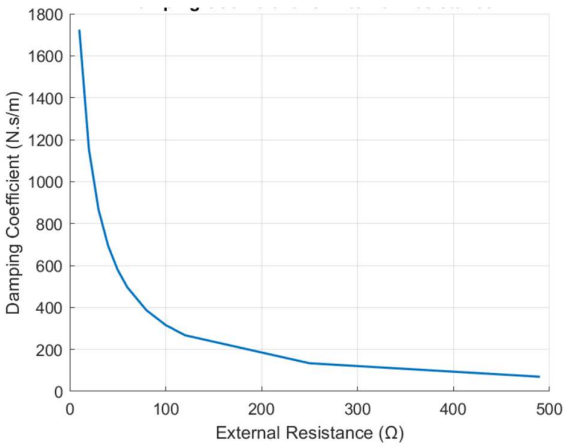

Fig. 2. Variation of damping coefficient as a function of the external electric resistance.

The variation of the external resistance directly affects the system's equivalent damping coefficient. A lower external resistance translates into higher current flow in the system, which increases the electromagnetic damping effect due to the back EMF generated by the DC motor. The result is a higher overall damping coefficient. On the other hand, a higher external resistance reduces the current flow, lowering the electromagnetic damping effect and hence the overall damping coefficient.

The simulation results in Figure 3 illustrate the recovered power as a function of the external resistance for different values of sprung mass and spring constants, comparing the hard spring constant (Figures 3 a, b) and the soft spring constant (Figures 3 c, d) values. The results shown in Fig.3 are obtained using four resonant frequencies for the external excitation. The figure highlights the impact of these parameters on the system's ability to generate power. The y-axis is presented on a logarithmic scale to reflect the wide range of power values.

In addition, the resonant frequency f_n and pulsation ω_n of every given sprung mass is displayed in Table 2. Only a subset of the obtained results has been displayed in the paper.

Table 2. Resonant frequency and pulsation of sprung masses

	Total spring constant soft (k_{soft})		**Total spring constant hard (k_{hard})**	
Mass (kg)	ω_n (rad/s)	f_n (Hz)	ω_n (rad/s)	f_n (Hz)
16	18.36	2.92	47.86	7.61
24	16.42	2.61	42.81	6.81
100	9.64	1.53	25.14	4.00
200	7.06	1.12	18.42	2.93
250	6.37	1.01	16.60	2.64
300	5.84	0.92	15.23	2.42
500	4.57	0.72	11.92	1.90
600	4.18	0.66	10.90	1.73

The resonant frequency of the system varies as a function of the sprung mass and spring constant according to the relationship: $\omega_n = \sqrt{\frac{k}{m_{eq}}}$

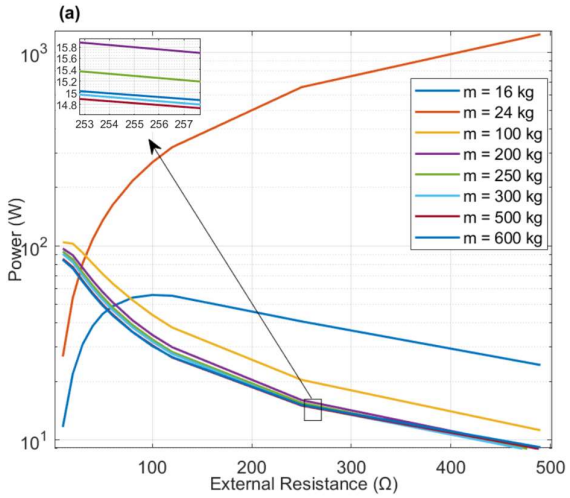

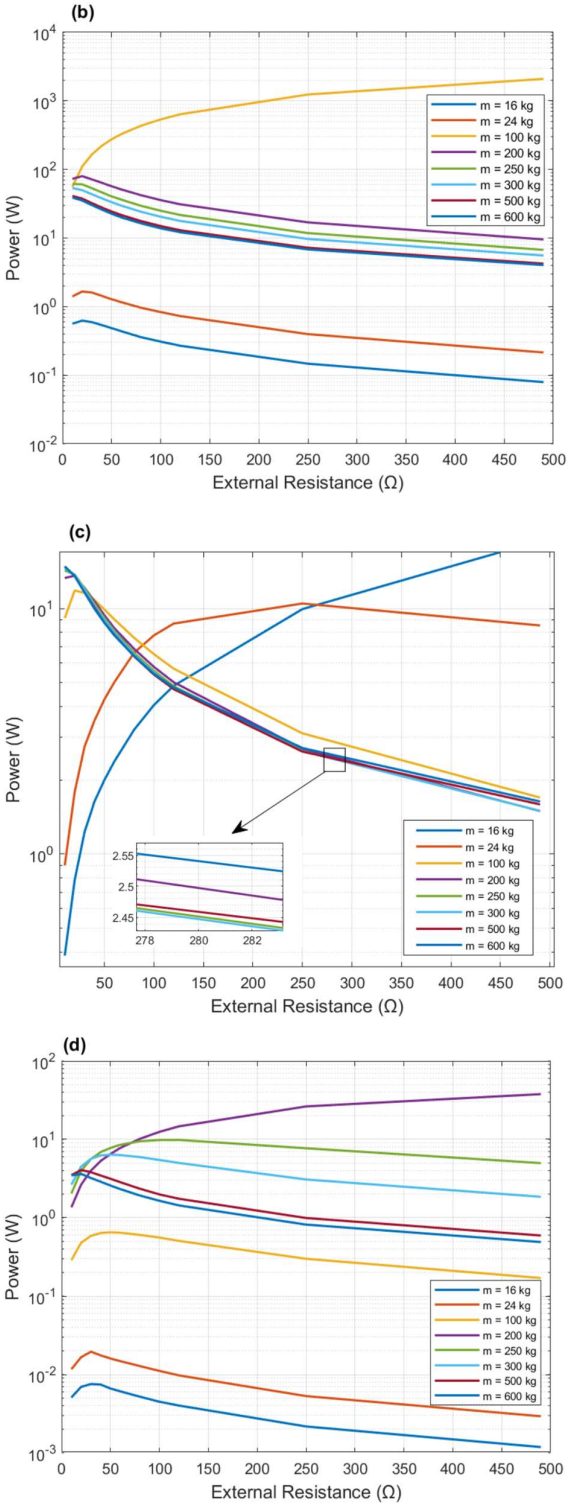

Fig. 3. Harvested Power vs external resistance for different sprung masses and different frequencies: Hard Spring constant k_{hard}(a) f=6.81 Hz; (b) f=4 Hz; Soft spring constant k_{soft} (c) f=2.92 Hz, (d) f=1.12 Hz.

Resonance occurs when the natural frequency aligns with the excitation frequency. In actual driving conditions, vehicles are subjected to vibrations over a range of excitation frequencies, mainly influenced by road surface irregularities, tire dynamics and vehicle speed. For passenger vehicles on typical road surfaces, the excitation frequency of the road increases with vehicle speed and decreases with the wavelength of the road roughness; excitation frequencies from 0.1 to 0.5 Hz are important for the assessment of motion sickness, and the range from 0.5 to 100 Hz is recommended for the driving comfort [11].

As shown in Fig.3, when the system frequency corresponds to the resonance frequency for each value of mass, the system is in resonance. Resonance leads to significant oscillations, which in turn can significantly increase output power. The amplitude of the oscillations increases significantly, leading to higher velocities of ball screw, then the increased velocity translates into higher current and consequently higher output power compared to non-resonant cases, especially for specific resistance values where output power is maximized.

The power output is also a function of the external resistance. There is an optimal resistance range for which the power output is maximized. This optimal resistance shifts based on the resonant frequency and the mass, indicating a need for varying the external resistance to achieve the maximum efficiency.

In Fig.3a, case with the hard spring constant and a frequency excitation f=6.81 Hz, as the external resistance increases from a lower value, the power output also increases until it reaches the peak. The system features greater resonance effects with sprung mass equal to m= 24 kg, with more marked power peaks at an external resistance of approximately 490 Ω. The peak power is noted to be 1253 W, which is unrealistic for such energy harvesting systems but can be justified by the high excitation amplitude, neglect of frictional and damping losses, and the optimal resonance conditions assumed in the simulation. Indeed, mechanical losses in ball-screws and gearboxes, such as friction and backlash, have a significant impact on the damping force in energy harvesting suspension systems. Friction losses reduce the energy transferred to the harvester, thus diminishing the efficiency of the damper. Additionally, gearbox backlash introduces non-linear responses, weakening the system's ability to control oscillations [12,13]. Transmission inefficiencies further reduce shock absorber force, compromising ride comfort and vehicle stability. In Fig.3b, case with the hard spring constant and a frequency excitation f=4.00 Hz, the power output for heavier masses (100 kg and above) is significantly higher compared to the lighter masses (16 kg and 24 kg). Maximum power output is highest for the 100 kg mass, reflecting the fact that at the given resonant frequency and hard spring constant, this mass is closer to the optimum sprung mass for energy harvesting.

In Fig.3c, soft spring constant and a frequency excitation f=2.92 Hz, power peaks are less evident and occur at lower external resistance values for the heavier masses. Conversely, the two lighter masses show a higher maximum power output, with a peak occurring at a different resistance value. Specifically at 16 kg mass

where the output power reached approximately 19 W at internal resistance equal to 490 Ω. As for Fig.3d, with soft spring constant and excitation frequency f=1.12 Hz heavier masses are overdamped and maintain higher power output in comparison to lighter mass. For a mass of 200 kg, adjusting the external resistance to the maximum value will maximize output power, resulting in a maximum value equal to 37 W at the corresponding resonant frequency.

Meanwhile, larger masses produce higher power outputs, with respect to resonant frequencies indicating that system efficiency improves with larger masses due to higher inertia. In this way, the hard spring system is more efficient than the soft spring one at converting mechanical oscillations into electrical energy, particularly at higher frequencies and with larger masses. However, in real road Gillespie [14] described that a soft suspension contributes to ride isolation because the acceleration of the sprung mass was found to be minimal at lower natural frequencies. In this case, the sprung mass acceleration was found to be minimal at a natural frequency of 1 Hz. However, other practical considerations limit natural frequencies between 1 and 1.5 Hz for most vehicles. The natural frequency for performance cars, where vehicle handling is more important than ride comfort, is between 2 and 2.5 Hz. Correct estimation of these frequencies is very important. Anyway, comfort considerations about the passengers of the vehicle should be carefully taken into account.

4 Conclusion

The parametric numerical simulations provided valuable insights into the optimization of the EHSA system for maximum energy efficiency. While output parameters such as output voltage, power and conversion efficiency provide valuable indicators of system performance, understanding and optimizing input parameters is crucial to achieving these results efficiently.

According to this study, spring stiffness (hard and soft) and damping coefficients directly influence the system's response to vibration. Further, the resistive load connected to the system has a direct impact on the electrical power generated. Higher electrical resistances can increase the amount of generated electrical energy. The study also highlights the importance of considering the interaction between sprung mass and resonant frequencies. Adjusting the mass to resonance frequencies can lead to resonance conditions that amplify the vibration amplitude, thus maximizing the output energy harvested by the system. This effect is particularly marked with larger masses. Nonetheless, comfort of the passengers of the vehicle is to be considered, which could result in lower energy harvesting of the system.

Nomenclature:

A: amplitude of excitation.

c_{eq}: Equivalent damping coefficient.

d: coefficient of the ball screw transformation.

F_b: output force of the ball screw.

f_n: resonant frequency.

J_m: inertia of the motor.

J_b: inertia of the ball screw.

J_g: inertia of the gearbox.

k: spring constant.

k_t: torque constant.

k_e: back EMF coefficient.

k_g: transmission ratio of the gearbox.

l: lead ratio of the ball screw.

m: sprung mass.

m_{eq}: Equivalent mass.

R_{load}: load resistance.

R_{int}: internal resistance of DC motor.

V_{emf}: back EMF voltage.

$x, \dot{x}, \ddot{x}$: displacement, velocity, acceleration of the sprung mass.

$z, \dot{z}, \ddot{z}$: stroke displacement, velocity, acceleration of the shock absorber.

$y, \dot{y}, \ddot{y}$: displacement, velocity, acceleration of base excitation.

$\theta, \dot{\theta}, \ddot{\theta}$: angular displacement, velocity, acceleration of the motor gear shaft.

η_g: efficiency of the gearbox.

η_b: efficiency of the ball screw.

τ_b: output torque of the shock absorber.

τ_i: output torque of the motor.

ω: excitation pulsation.

ω_n: resonant pulsation.

References

1. R. Zhang, X. Wang, S. John, A comprehensive review of the techniques on regenerative shock absorber systems, Energies. **11**, 1167 (2018).
2. M. A A. Abdelkareem, L. Xu, M. K. A. Ali, A. Elagouz, J. Mi, S. Guo, Y. Liu, L. Zuo, Vibration energy harvesting in automotive suspension system: A detailed review, Appl. Energy. **229**, 672-699 (2018).
3. L. Qi, H. Pan, Y. Pan, D. Luo, J. Yan, and Z. Zhang, A review of vibration energy harvesting in rail transportation field, IScience .**25**, 103849 (2022).
4. R. Zhou, M. Yan, F. Sun, J. Jin, Q. Li, F. Xu, M. Zhang, X. Zhang, K. Nakano, Experimental validations of a magnetic energy-harvesting suspension and its potential application for self-powered sensing, Energy. **239**, 122205 (2022).
5. M. Abdelrahman, G. Liu, C. Fan, Z. Zhang, A. Ali, H. Li, A. Azam, H. Cao, A. A. Mohamed,

Energy regenerative shock absorber based on a slotted link conversion mechanism for application in the electrical bus to power the low wattages devices, Appl. Energy.**347**, 121409 (2023).

6. Z. Wang, T. Zhang, Z. Zhang, Y. Yuan, Y. Liu, A high-efficiency regenerative shock absorber considering twin ball screws transmissions for application in range-extended electric vehicles, Energy. Built. Environ. **1**, 36-49 (2020).
7. W. Zhang, G. Wang, Y. Guo, Research on damping and energy recovery characteristics of a novel mechanical-electrical-hydraulic regenerative suspension system, Energy. **271**, 127022 (2023).
8. B. Huang, C.-Y. Hsieh, F. Golnaraghi, M. Moallem, A methodology for optimal design of a vehicle suspension system with energy regeneration capability, J. Vib.Acoust. **137**,051014 (2015).
9. B. Huang, C.-Y. Hsieh, F. Golnaraghi, M. Moallem, Development and optimization of an energy-regenerative suspension system under stochastic road excitation, J. Sound. Vib. **357**, 16-34 (2015).
10. International Standardization Organization, ISO 2631-1:1997, Mechanical vibration and shock — Evaluation of human exposure to whole-body vibration — Part 1: General requirements, Iso.org, (2017): https://www.iso.org/obp/ui/en/#iso:std:iso:2631:-1:ed-2:v2:en.
11. C. V. Suciu, T. Tobiishi, and R. Morii, Modeling and Simulation of a Vehicle Suspension with Variable Damping versus the Excitation Frequency,J. Telecommun. Inf. Technol. 83-89 (2012).
12. G. A. Ambaye, The Performance of Gear with Backlash: A Review, J.Appl.Mech.Eng. **10**, 389 (2021).
13. Li, Z., Brindak, Z., Zuo, L., "Modeling of an Electromagnetic Vibration Energy Harvester with Motion Magnification," *Proceedings of the ASME International Mechanical Engineering Congress and Exposition: Dynamic Systems and Control; Mechatronics and Intelligent Machines, Parts A and B*, Denver, Colorado, USA, 2011.
14. T.D. Gillespie, Fundamental of Vehicle Dynamics, (SAE International, 1992)